Solid State Phenomena
ISSN: 1662-9779, Vol. 388, pp 141-151
doi:10.4028/p-iS64g3

Submitted: 2026-01-19
Revised: 2026-02-12
Accepted: 2026-02-17
Online: 2026-04-15

Forming Limit Test of Asymmetric Al-Polymer Laminate Composite Film

Cheol Sagong[1,a], Taek Jin Jang[2,b], Taegyun Ahn[1,c] and Jeong Whan Yoon[1,3,d*]

[1]Department of Mechanical Engineering, Korea Advanced Institute of Science and Technology, 291 Daehak-ro, Science Town, Daejeon 34141, Republic of Korea

[2]SK On, 325, Expo-ro, Yuseong-gu, Daejeon, Republic of Korea

[3]School of Engineering, Deakin University, 75 Pigdons Rd., Waurn Ponds, VIC 3216, Australia

[a]sak9709@kaist.ac.kr, [b]taekjin.jang@sk.com, [c]t.ahn@kaist.ac.kr, [d*]j.yoon@kaist.ac.kr

Keywords: al-polymer laminate composite film, forming limit, modified marciniak test, polar effective plastic strain (PEPS) approach.

Abstract. As environmental issues arise, increasing battery efficiency is emerging as an important task. To manufacture more efficient lithium-ion batteries, the industry is striving to increase the depth of battery cell. A growing number of companies are focusing on developing pouch-type batteries using materials with high formability. To produce the battery cell with bigger depth, understanding of the formability of the material is important. Forming limit test can be considered. The material used in pouch-type batteries is an asymmetric aluminum-polymer laminate composite, which consists of four layers: polypropylene, aluminum, nylon, and PET. Because of the good formability of the polymer layers, a forming limit curve cannot be obtained using typical forming limit test such as experiment using Nakazima specimen. Therefore, the modified Marciniak testing method is implemented in this research, which is helpful for inducing strain concentration in the middle of the specimen. In the modified Marciniak test, a dummy sheet is layered between the specimen and the punch, to prevent the fracture around the region contacting with the fillet of the punch. In this research, different kinds of polymers were tried as the dummy sheet material. In addition, specimens of various designs were tested and the forming limit test results of the Al-Polymer film with thickness of 153\mu m were converted using the Polar Effective Plastic Strain (PEPS) approach.

1. Introduction

With the global trend toward carbon emission regulations, interest in electric vehicles (EVs) has increased significantly, and the automotive industry is undergoing a rapid transition toward an EV-centered industrial structure. Accordingly, numerous companies are actively developing technologies aimed at improving the efficiency of lithium-ion batteries used in electric vehicles. There are three types of battery cells-cylindrical, prismatic and pouch types. Especially, because of the excellent formability of the pouch-type battery material (Al-Polymer film), it is possible to obtain superior energy efficiency. In addition, the shape of the pouch-type battery cell is similar to that of the prismatic one, and therefore it can also benefit in terms of spatial efficiency. Thus, pouch-type cells are the primary focus of the present study.

To enhance the energy efficiency of the battery cells, the forming depth should be increased. However, some defects such as wrinkling and fracture can occur during the forming process. To prevent these defects, it is essential to identify the proper forming condition through numerical simulation. For finite element simulation of the process, constitutive models and forming limit curves (FLCs) of the material must be established first. The raw material of the pouch-type battery cell is a 4-layer laminated composite film and four different materials are polypropylene, aluminum, nylon and PET as illustrated in Fig. 1. Because of this complicated structure, relatively limited research has been conducted on experimental investigation and material modeling. Jang et al.[1] developed material models based on optimization. In addition, Moon et al.[2] obtained the properties of each individual layer by physically separating the pouch film.

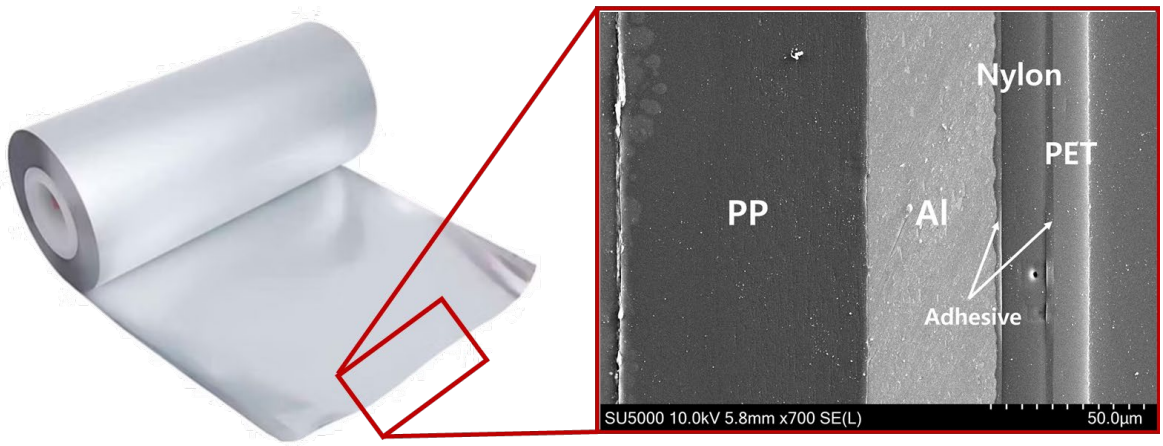

Fig. 1. Cross-sectional view of pouch film.

However, because of the superior formability of the material, determining the forming limit curve experimentally is a highly challenging problem. Moon et al.[3] established a forming limit curve using the Nakazima test. However, strain localization did not occur at the center of the specimen for some cases. In addition, during the forming limit test for the nylon/PET layers, nonlinear strain paths were observed. Forming limit curves are sensitive to strain paths, and therefore these issues prevent to obtain the accurate FLC of the material.

In the present study, conventional forming limit testing methods such as the Marciniak test [4] and the Nakazima test [5] were first conducted. Based on these experimental results, the limitations of these conventional methods were identified. Subsequently, the testing method was improved based on the modified Marciniak test proposed by Bong et al. [6]. To avoid the strain path nonlinearity problem, circular specimens proposed by Kim et al. [7] were employed. Furthermore, to overcome the excellent formability induced by the polymer layers in the pouch film, dummy sheets were fabricated using a type of polymer material, EPDM. Finally, to address the remaining strain-path nonlinearity, the polar effective plastic strain (PEPS) approach proposed by Stoughton and Yoon [8] was implemented.

2. Test Results for Conventional Forming Limit Test

As an initial phase of the investigation, conventional forming-limit testing methods, specifically the Marciniak and the Nakazima tests were implemented. As illustrated in Fig. 2(a), a flat-headed punch is employed in the Marciniak test. This configuration allows strain localization to occur at the central region; however, it is also prone to generating frictional stresses on specific region of the specimen which is contacting the punch's fillet. In contrast, the Nakazima test (Fig. 2(b)) incorporates a hemispherical punch, thereby avoiding the excessive fillet-induced strain concentration. Owing to the shape of the punch, it is possible to induce the more homogeneous deformation then in the Marciniak test. However, necking can be initiated after a comparatively larger punch displacement.

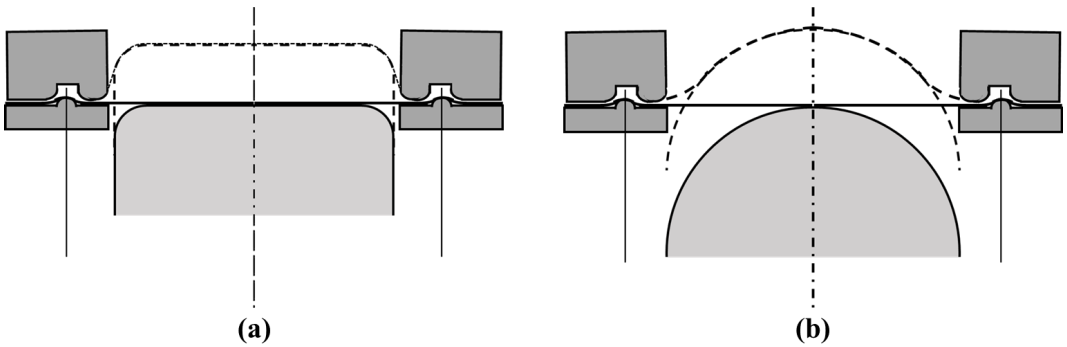

Fig. 2. Schematic of conventional forming limit test (a) Marciniak test (b) Nakazima test.

Through the DIC image of the Marciniak test (Fig. 3), it can be confirmed that deformation is predominantly concentrated in the punch-fillet region from the very early stage of the test. This is the result of excessive friction nearby the punch's fillet and this friction impeded deformation in the central area of the specimen. As a result, localized necking is initiated at the fillet, thereby preventing the acquisition of meaningful forming-limit data along the intended strain path.

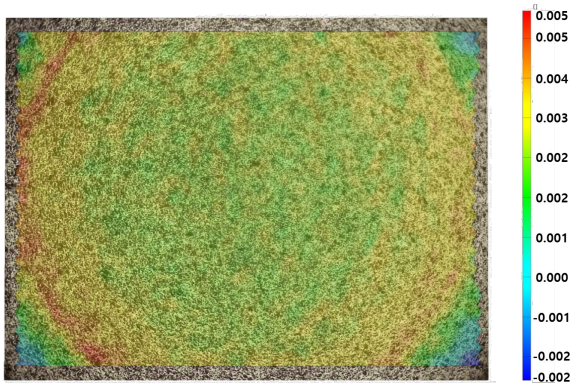

Fig. 3. DIC image of Marciniak test in very early stage (major strain).

Fig. 4 displays the DIC results from the Nakazima test. Although the hemispherical punch suppressed initial strain concentration which is observed in the Marciniak test, localization instead occurred along the specimen edges prior to the initiation of central necking. This behavior is attributed to the exceptionally high formability of the pouch film, which allowed the punch to advance excessively until its tip became exposed. As illustrated in Fig. 5, the direct contact between the punch tip and the specimen induced localized deformation, and this inhibited the development of necking in the central region. Consequently, similar to the Marciniak test, the experiment could not be successfully completed. The fractured Nakazima specimens are shown in Fig. 6.

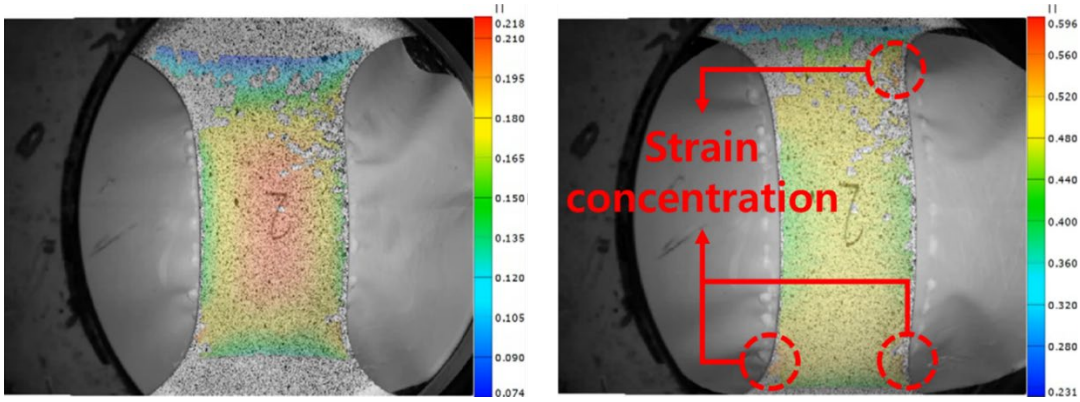

Fig. 4. DIC image of Nakazima test (major strain).

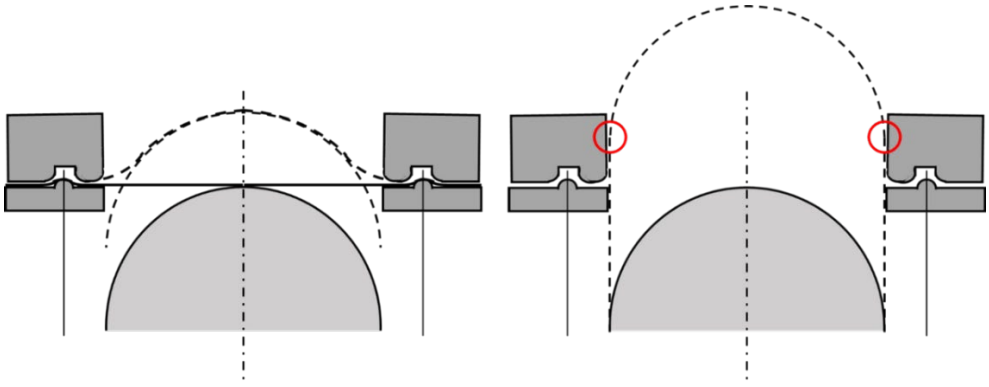

Fig. 5. Nakazima punch's crack tip.

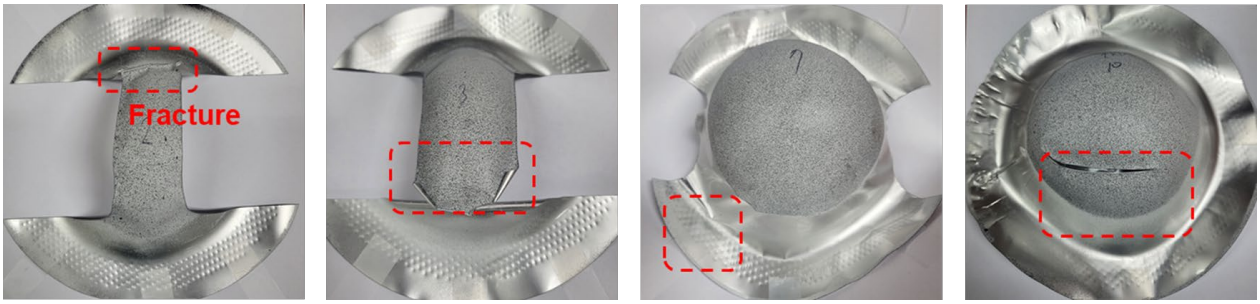

Fig. 6. Specimens after Nakazima test.

3. Development of Testing Method

Based on the experimental results and analyses of both conventional forming-limit test methods, the Marciniak testing method was modified in this study. Following the methodology proposed by Bong et al.[6], a dummy sheet was introduced, and the circular-shaped specimen geometry was implemented as recommended by Kim et al [7]. In addition, the polymer-made dummy sheet material was employed, to enable the establishment of forming-limit test conditions suitable for obtaining reliable results from thin films with superior formability. The configuration of the tool used in the test is illustrated in Fig. 7.

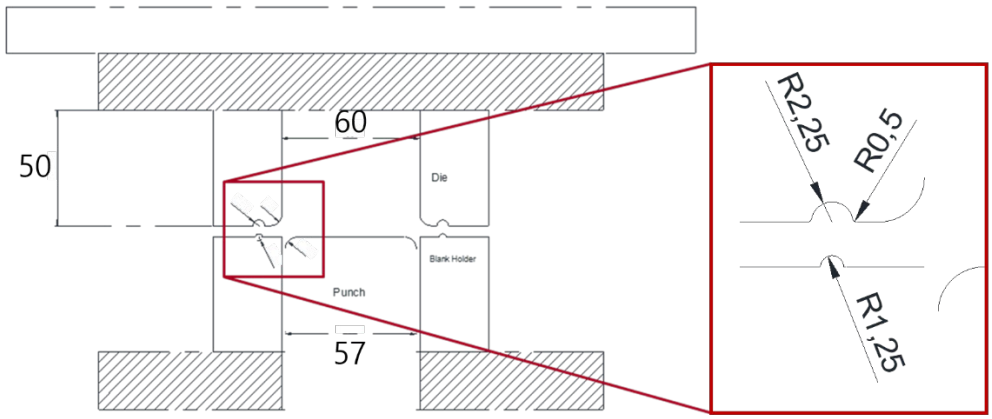

Fig. 7. Geometry of forming limit testing tool [mm].

Modified Marciniak Test with Dummy Sheet Made of Stainless Steel.

To avoid the challenges observed in the Nakazima test arising from the material's high formability, a modified Marciniak test was implemented to induce strain localization at the center of the specimen. Bong et al. [6] developed this modified approach as an improvement to the conventional Marciniak test, and they implemented the specimen geometry proposed by Raghavan [9]. In their experiment, a dummy sheet was placed between the punch and the specimen to reduce excessive strain accumulation near the punch fillet, while the friction between the dummy and the specimen made dragging possible. Additionally, a lubricant was applied between the dummy sheet and the punch to minimize friction around the fillet-contacting region. The underlying principle of the modified Marciniak test is illustrated in Fig. 8, with the specimen geometry detailed in Bong et al.[6], where a 1 mm-thick stainless steel sheet served as the dummy sheet. A circular hole was introduced at the center of the dummy sheet so that, during deformation, only the specimen area in direct contact with the dummy was dragged, thereby inducing strain localization in the central region of the specimen.

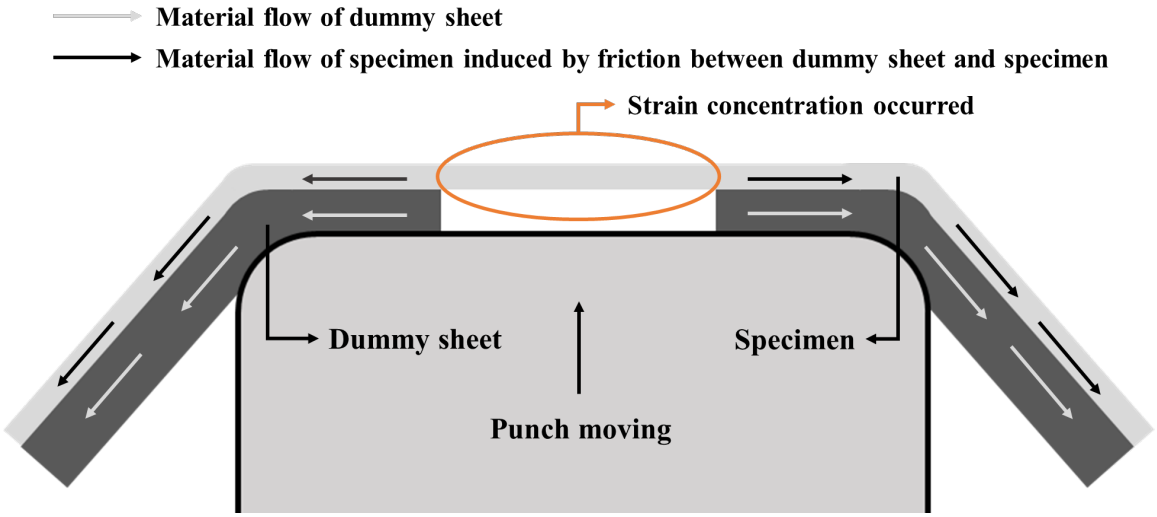

Fig. 8. Schematic of Modified Marciniak test.

Similarly, the modified Marciniak test was performed on the pouch film using a stainless steel dummy sheet. Fig. 9 illustrates the deformation of the stainless steel dummy sheet and the specimens across strain states ranging from uniaxial tension to plane strain on the forming-limit diagram. As illustrated in Fig. 9(a), the dummy sheet underwent uniaxial tension in one direction and compression in the perpendicular direction, leading to wrinkling and bulging. Consequently, as shown in Fig. 9(b), deformation occurred around the dummy sheet hole rather than at the specimen center. For tests along the equi-biaxial path, fracture initiated at the hole edge of the dummy sheet before specimen necking, preventing the acquisition of reliable forming-limit data. The fractured dummy sheet and corresponding specimen are presented in Fig. 10.

(a) (b)

Fig. 9. Deformation of dummy sheets and specimen from uniaxial tension to plane strain.

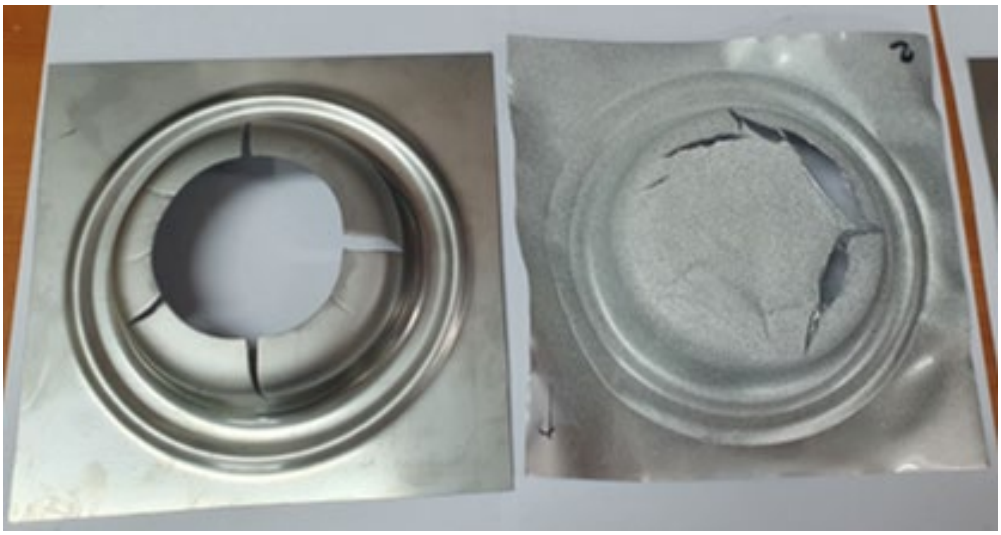

Fig. 10. Failure of dummy sheet and specimen in equi-biaxial loading.

Specimen Design Study.

Using the Raghavan specimen, the non-uniform radial distance from the center to the edge led to sensitivity to the blank holding force, as confirmed by repeated trials. In the plane strain region, nonlinear behavior was observed. Since the forming limit can be affected by the strain paths, path linearity is essential. To maintain the strain path linearly, the circular specimen design proposed by Kim et al. (Fig. 11(a)) [7] was adopted, and as shown in Fig. 11(b), it produced slightly more linear strain paths compared to the Raghavan specimen. In Fig. 11(b), the test results labeled as "Kim et al." were obtained using the width-60 specimen shown in Fig. 11(a), whereas the test results labeled as "Raghavan" were obtained using the plane strain specimen design proposed by Bong et al.[6].

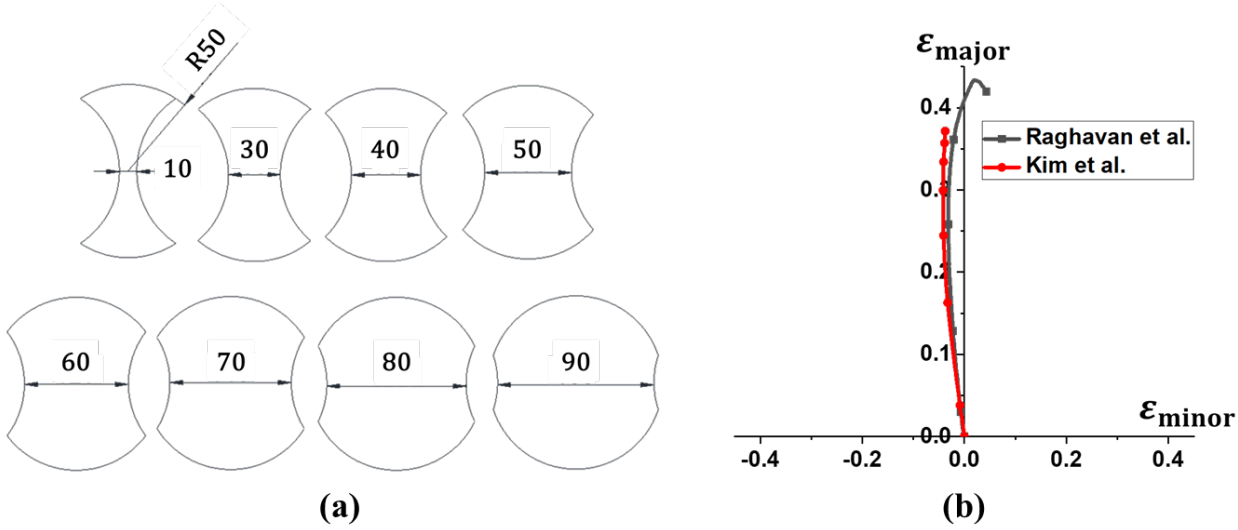

Fig. 11. (a) Kim et al's specimen [7] (b) Paths' nonlinearity change by specimen design.

Dummy sheets' material.

Due to the limitations of stainless steel as a dummy sheet, materials with higher formability and lower stiffness were employed. Three polymers were selected: 1.0 mm-thick silicone, 1.4 mm-thick urethane, and 1.6 mm-thick EPDM. Uniaxial tensile tests (Fig. 12(a)) confirmed that all candidates exhibited very high elongation. The dummy sheets fabricated using these polymers are shown in Fig. 12(b) and Fig. 12(c).

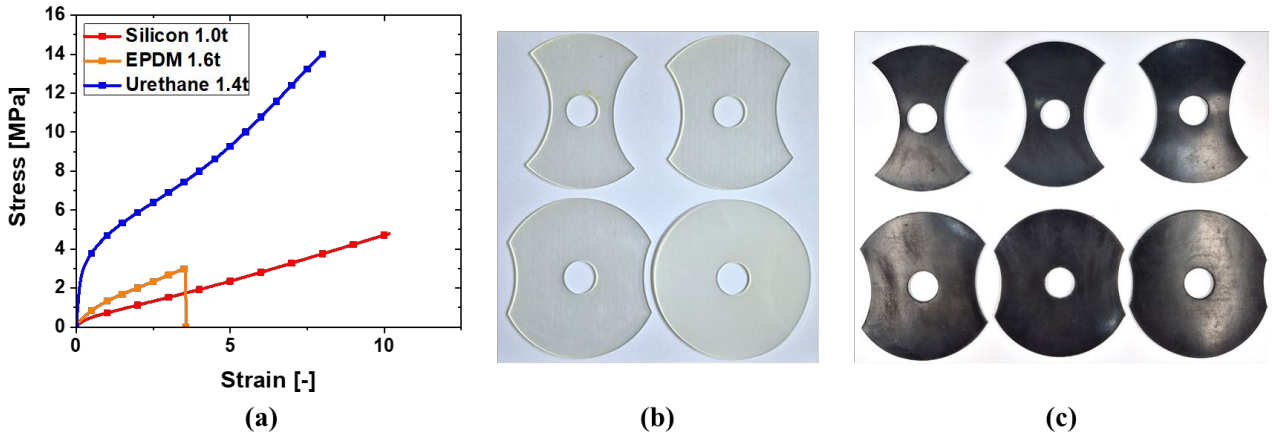

Fig. 12. (a) Result of uniaxial tension of polymer (b) Urethane dummy sheets (c) EPDM dummy sheets.

Test results indicated that the stiffness of urethane is much higher compared with that of the pouch film, causing strain localization near the edge of the dummy sheet hole, similar to the stainless steel case. In contrast, using EPDM enabled successful central strain localization across all strain paths with fracture consistently occurring at the specimen center for every strain path (Fig. 13).

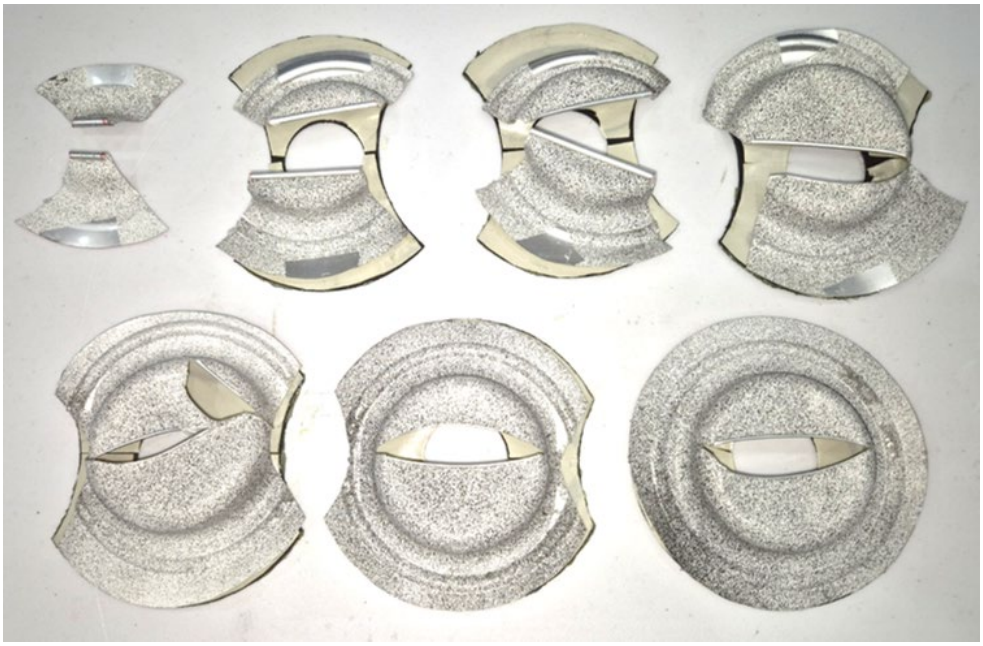

Fig. 13. Fractured specimens after forming limit test results with EPDM dummy sheets.

4. Test Results

Forming-limit tests conducted using this method showed that, while deformation was successfully localized at the specimen center, strain paths from the plane strain to the equi-biaxial regions remained strongly nonlinear (Fig. 14). The degree of nonlinearity is too pronounced to be approximated as linear, complicating accurate forming-limit curve determination and necessitating the introduction of a correction method.

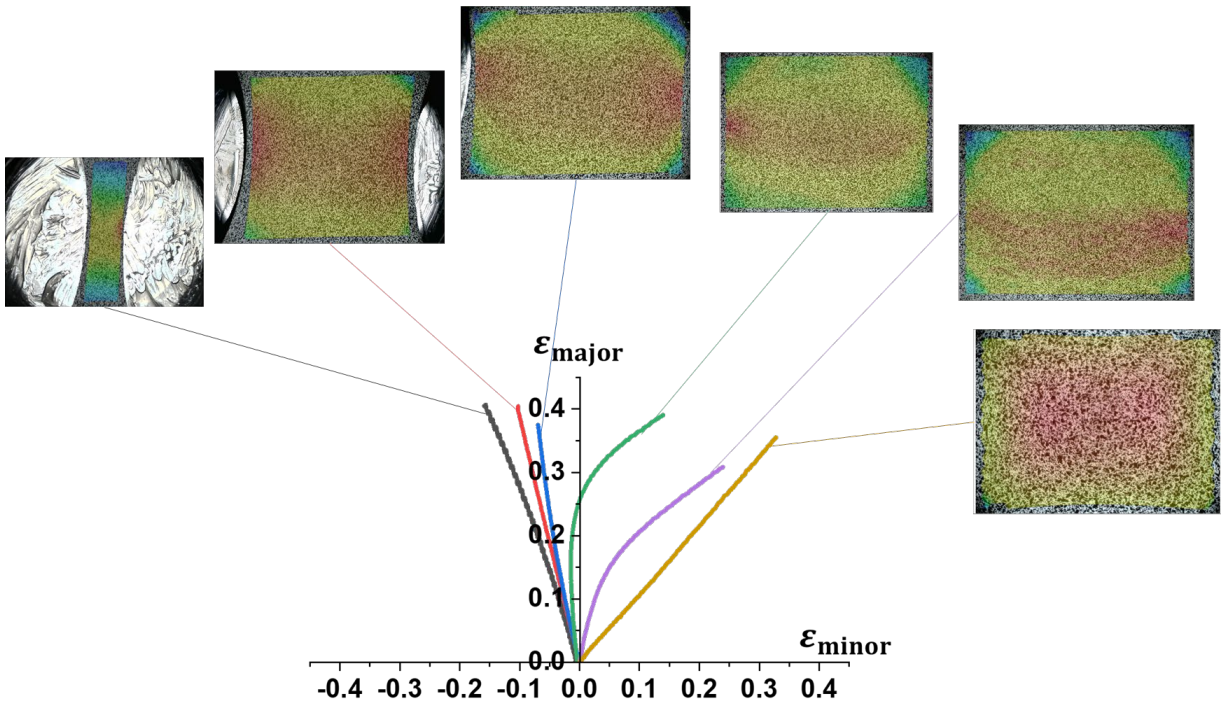

Fig. 14. Nonlinearity of strain paths.

To address this issue, the forming-limit curve was converted using the path-independent approach based on Polar Effective Plastic Strain (PEPS), as developed by Stoughton and Yoon [8]. The PEPS method transforms the conventional forming-limit diagram, defined in terms of major and minor

strains, into a polar coordinate system based on the magnitude and orientation of strain increments (Fig. 15). For the normal anisotropic model, the effective plastic strain is calculated as

$$\bar{\varepsilon}_p = \frac{1+r}{\sqrt{1+2r}} \int \sqrt{\dot{\varepsilon}_1^2 + \dot{\varepsilon}_2^2 + \frac{2r}{1+r}\dot{\varepsilon}_1\dot{\varepsilon}_2}\, dt \tag{1}$$

and the angle for the increment, θ is calculated as

$$\theta = \tan^{-1}\left(\frac{\dot{\varepsilon}_2}{\dot{\varepsilon}_1}\right) \tag{2}$$

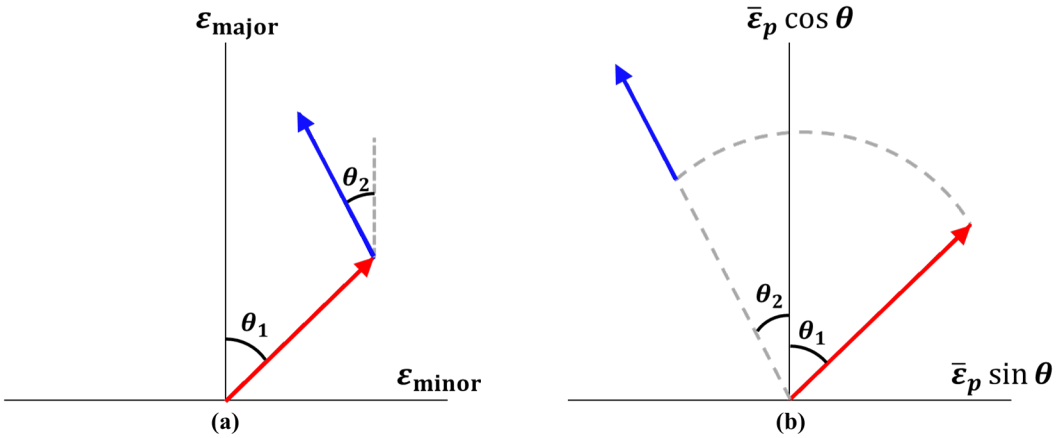

Fig. 15. Schematic of PEPS approach (a) path sensitive FLD on major-minor strain coordinate (b) path-independent polar effective plastic strain diagram.

where r is the r-value(the Lankford coefficient) of the material. This enables the construction of a path-independent forming limit curve. Since the experiments in this study were performed along the transverse direction, the TD r-value was adopted in the PEPS formulation. The r-values in each direction were obtained from uniaxial tensile tests, and the corresponding values are summarized in Table 1. In addition, Fig. 16 presents the results of the uniaxial tensile tests conducted along different directions of the pouch film.

Table 1. Lankford coefficients in each direction.

RD	DD	TD
0.723	1.256	0.828

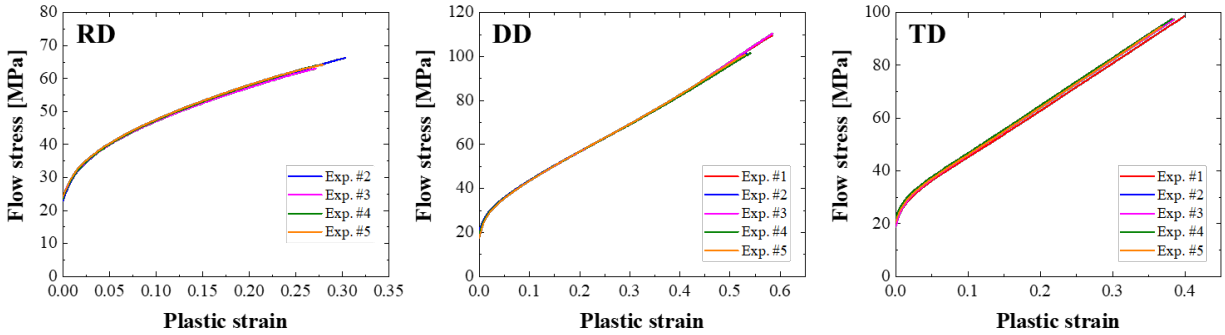

Fig. 16. Stress-strain curves of the pouch film.

In this study, forming-limit test results obtained from nonlinear strain paths were converted using the PEPS-based polar coordinate system, and they are represented in the Fig. 17.

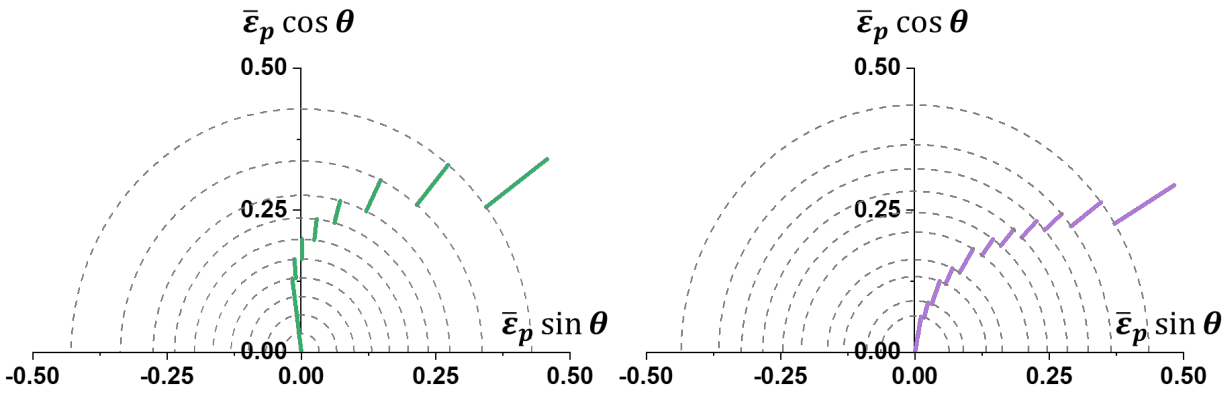

Fig. 17. Nonlinear paths in PEPS-based polar coordinate system.

Fig. 18 (a) shows the results of the PEPS-based analysis applied to all experimental results, including those with linear strain paths. The reconverted FLD into strain space without the elements over the biaxial range is represented in Fig. 18 (b). In addition, the forming limit curve obtained after excluding elements beyond the biaxial region was also plotted.

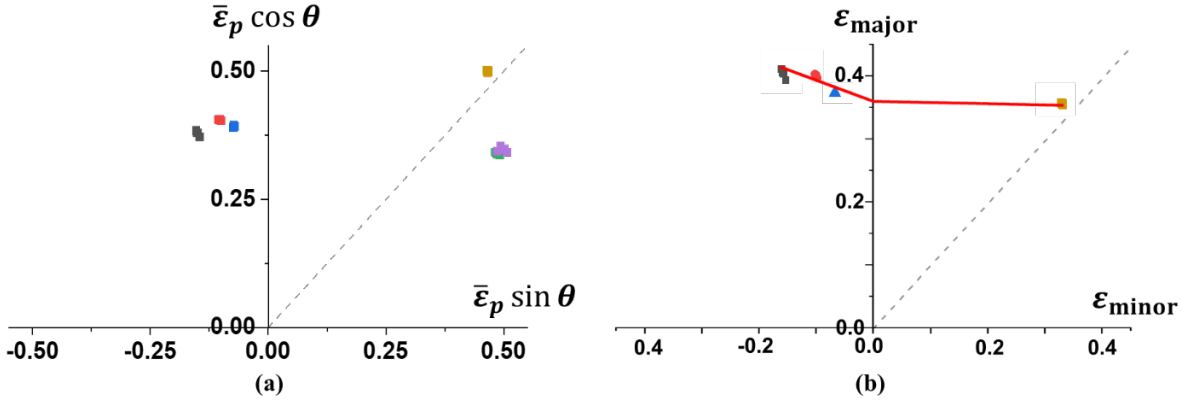

Fig. 18. (a) FLD converted using PEPS approach (b) Reconverted FLD into strain space by excluding the elements over the biaxial range.

5. Discussion

Among the elements shown in Fig. 18(b), the data corresponding to the region from uniaxial tension to plane strain followed linear strain paths and were therefore included in the construction of the forming limit curve. In contrast, the elements located between the plane strain and the equi-biaxial regions exhibited nonlinear strain paths and were thus excluded, as they are not suitable for defining the forming limit curve in strain space. After excluding these elements, the resulting trend shows a decrease in major strain with increasing minor strain, which is consistent with the behavior commonly observed in most thin sheet metal materials.

Notably, Moon et al.[6] reported that nonlinear strain paths were observed even when forming limit tests were conducted using specimens composed solely of nylon and PET layers[3], without the polypropylene and aluminum layers. By interpreting this observation, the nonlinear strain paths are strongly influenced by the differences in the mechanical behavior of the layers – not only between the metal and polymer, but also between the polymer layers.

Strain-rate sensitivity and viscoelastic-plastic behavior are important behaviors which are observed in polymers, and these characteristics can affect the strain increment. In principle, forming limits should be determined based on plastic deformation; however, even after the aluminum has started the plastic deformation, the polymer may have continued to undergo non-negligible elastic deformation and this can be one of the reasons for a nonlinear strain path. In addition, the presence of weak or partially degraded interfaces may promote interlayer sliding or delamination during forming, further

complicating the strain evolution. These interfacial phenomena can locally relax in-plane constraints and redistribute strains, and thus the biaxial-dominant modes deformation can be induced. Therefore, to explain the strain-path nonlinearity of the pouch film, the interaction between each layer should be considered along with the layers' material properties as well.

Even though the elements beyond the biaxial range were excluded using the PEPS approach, further research is necessary to obtain data in the region between plane strain and equi-biaxial tension. Future work will be extended beyond geometric specimen optimization, polymer layer's constitutive behavior and interlayer delamination mechanisms into both experiment and numerical modeling. Designing a novel specimen that enables maintenance of deformation modes in biaxial tensile loading is essential. In addition, integrating such advanced material modeling with specimen design optimization and the PEPS-based framework is expected to enable the construction of a complete and physically consistent forming limit curve for the pouch film.

6. Conclusion

In this study, the forming limit of pouch-type battery films was investigated through conventional and modified forming limit tests. In addition, the nonlinear strain-path of the material was emphasized. Conventional forming limit tests were first conducted, and it was identified the limitation of these tests in preserving strain linearity during testing were identified. Based on these test results, the modified Marciniak testing method was implemented, with circular specimens and EPDM dummy sheets to suppress undesired deformation and enhance strain localization in the center.

To transform the forming limit data, which show the nonlinear strain paths, into a path-independent framework, the polar effective plastic strain (PEPS) approach was implemented. However, in the region between plane strain an equi-biaxial tension, it was not able to construct the forming limit due to the critical limitations of the PEPS method. The major strain increment became smaller than the minor strain increment as the test proceeded, driving the strain state beyond the equi-biaxial region.

The present results demonstrate that strain-path nonlinearity in the material cannot be fully explained by specimen geometry or metal-polymer interactions alone. According to the experimental results showing nonlinear strain paths in nylon-PET-only specimens conducted by Moon et al[6], it is evident that interlayer delamination mechanisms are governing strain evolution. Therefore, it should be interpreted that the difficulty in obtaining the FLC arises from the fundamental limitation of current forming limit testing methods, rather than the limitation of the PEPS.

For future work, the development of novel specimen designs will be focused on inducing desired linear deformation modes between plane strain and biaxial tensile region. In parallel, advanced material modeling incorporating strain-rate-dependent and interlayer delamination behavior will be pursued to enable more accurate interpretation of experimental strain paths. The integration of experiments and material modeling is expected to provide a more comprehensive and physically consistent forming limit description. Therefore, the predictive capability of forming simulations for pouch-type battery cell manufacturing processes can be improved.

Acknowledgement

This work was supported by Basic Science Research Program through the National Research Foundation of Korea (NRF) funded by the Ministry of Education (RS-2025-25406725). This work is also partially supported by Materials and Components Technology Development Program (RS-2024-00432591) funded by the Ministry of Trade, Industry and Resources (MOTIR, Korea).

References

[1] Jang, T. J., Sagong, C., Ahn, T., & Yoon, J. W. (2024). Characterization of layered anisotropic properties for Li-ion battery pouch film and its application to forming. CIRP Annals, 73(1), 225-228.

[2] Moon, C., Lian, J., & Lee, M. G. (2023). Identification of elastic and plastic properties of aluminum-polymer laminated pouch film for lithium-ion batteries: A hybrid experimental-numerical scheme. Journal of Energy Storage, 72, 108601.

[3] Moon, C., hyeon Park, J., Lian, J., Lee, H. L., Ma, J., & Lee, M. G. (2025). Formability of PET/PA/Al/PP laminated composite pouch for Li-ion battery: Analysis based on experiments and modeling. Journal of Power Sources, 653, 237746.

[4] Marciniak, Z. & Kuczy'nski, K. (1967). Limit strains in the processes of stretch-forming sheet metal, International journal of mechanical sciences, 9(9) 609-620.

[5] Nakazima, K., Kikuma, T. & Hasuka, K. (1968). Study on the formability of steel sheets, Yawata Technical Report, 264, 8517-8530.

[6] Bong, H. J., Barlat, F., Lee, M. G., & Ahn, D. C. (2012). The forming limit diagram of ferritic stainless steel sheets: Experiments and modeling. International Journal of Mechanical Sciences, 64(1), 1-10.

[7] Kim, S. B., Huh, H., Bok, H. H., & Moon, M. B. (2011). Forming limit diagram of auto-body steel sheets for high-speed sheet metal forming. Journal of Materials Processing Technology, 211(5), 851-862.

[8] Stoughton, T. B., & Yoon, J. W. (2012). Path independent forming limits in strain and stress spaces. International Journal of Solids and Structures, 49(25), 3616-3625.

[9] Raghavan, K. S. (1995). A simple technique to generate in-plane forming limit curves and selected applications. Metallurgical and materials transactions A, 26(8), 2075-2084.